Faint blue galaxies: high or low redshift?

Matthew Colless,[1] Richard S. Ellis,[2] T. J. Broadhurst,[3] Keith Taylor[4] and Bruce A. Peterson[5]

[1] *Institute of Astronomy, Madingley Road, Cambridge CB3 0HA*
[2] *Physics Department, University of Durham, South Road, Durham DH1 3LE*
[3] *Royal Observatory, Blackford Hill, Edinburgh EH9 3HJ*
[4] *Anglo-Australian Observatory, PO Box 296, Epping, NSW 2121, Australia*
[5] *Mount Stromlo & Siding Spring Observatories, The Australian National University, Weston, ACT 2611, Australia*

ABSTRACT
The original LDSS deep redshift survey showed that the bulk of the faint blue galaxies brighter than $b_J = 22.5$ are at redshifts less than $z = 0.5$. However, the 19 per cent incompleteness of the survey left open the possibility that some small subset of the galaxy population may be at high redshift $(z > 0.7)$ and have subsequently undergone strong luminosity evolution. With new observations we have now reduced the incompleteness in two of the original survey zones to just 4.5 per cent. No galaxies with $z > 0.7$ were found, confirming the previous results. The 90 per cent confidence upper limit on the number of high-redshift galaxies brighter than $b_J = 22.5$ is consistent with no evolution but inconsistent with *any* significant luminosity evolution of $L > L^*$ galaxies. The 99 per cent limit is consistent with no more than 1.0–1.2 magnitudes of luminosity evolution by a redshift of $z = 1$. We have also carried out a deeper survey of the bluest galaxies with $22 < R < 23$. Redshifts were obtained for 11 out of 23 objects with $B - R \leq 0.70$ and/or $R - I \leq 0.75$. Most importantly, the redshifts of all six galaxies with $B - I < 1$, indicative of a near-flat spectrum in f_ν, were identified. Apart from one QSO, the identified objects all have $z < 1$. The observation that all the flat-spectrum objects are at low redshift rules out galaxy evolution models with mild luminosity evolution only (low q_0, high z_f), which predict that almost all galaxies with these colours should have $z > 1$. The luminosities of the galaxies with near-flat spectra span the range of $0.15L^*$ to $0.02L^*$, from normal galaxies to dwarfs. These results are consistent both with merging-dominated models for galaxy evolution and with models postulating bursts of star formation in dwarf galaxies. Infrared-selected redshift surveys and multicolour high-resolution imaging offer means to discriminate between these scenarios.

Key words: galaxies: distances and redshifts – galaxies: evolution – galaxies: formation – galaxies: luminosity function, mass function.

1 INTRODUCTION

Much of our understanding of galaxy evolution is based on studies of the numbers, colours and redshifts of galaxies at faint apparent magnitudes. The advent of CCD detectors over the past 10 years has meant that these observations have been extended to very faint limits. More recently the advent of multi-object spectroscopy has increased by an order of magnitude or more the number of redshifts that can be gathered in a given amount of telescope time. These technical advances have produced some surprising results. This paper addresses two important issues arising from recent studies of the distributions of colours and redshifts for faint galaxies.

The first follows from the deep redshift surveys of Broadhurst, Ellis & Shanks (1988) and Colless et al. (1990, hereafter Paper I) who used fibres and multislits respectively to gather a total of 274 redshifts for purely magnitude-limited samples of galaxies with $20 \leq b_J \leq 22.5$. In this magnitude range, the redshift distribution predicted by standard models

of galaxy luminosity evolution (Yoshii & Peterson 1991) has a tail extending to high redshift that is absent from the redshift distribution of no-evolution models, although the medians from both models are similar. The galaxies in this high-redshift tail are required by the standard models of galaxy luminosity evolution to explain the number counts, which are observed to be significantly greater than those predicted in the case of no evolution of the galaxy population. Yet, remarkably, the range of redshifts *observed* is consistent with no brightening at all of galaxies at the bright end of the galaxy luminosity function. The interesting question is how much luminosity evolution of $L \gtrsim L^*$ galaxies is *allowed* by the observations, and what this can tell us about the star-formation history of bright normal galaxies.

The constraints on the allowed amount of luminosity evolution for $L \gtrsim L^*$ are stronger from the fainter of the two studies, the LDSS deep redshift survey (Paper I), which reached $b_J = 22.5$. However, this survey yielded redshifts for only 81 per cent of the sample, leaving the possibility open that the unidentified objects were $L \gtrsim L^*$ galaxies at higher redshifts. In Paper I we argued, on the basis of the detectability of the [O II] 3727-Å line in the unidentified spectra, that the fraction of unidentified objects that could be at redshifts higher than the maximum observed redshift of $z \approx 0.7$ was small under the (reasonable) assumption that the redshift distribution declines monotonically with redshift (i.e. is not bimodal). Specifically we found that there was only a 2 per cent probability that all the unidentified objects (25 per cent of sample galaxies) were in an extended tail to the observed redshift distribution beyond $z = 0.7$.

The high-redshift tail of the redshift distribution is particularly sensitive to luminosity evolution of the brightest galaxies because the bright end of the luminosity function is so steep. A small amount of luminosity evolution can produce a large increase in the numbers of bright galaxies and a corresponding boost to the high end of the redshift distribution where they dominate. In Section 2 we describe new observations with the Low Dispersion Survey Spectrograph (LDSS) aimed at completing and extending the original sample of Paper I in order to tie down the tail of the $b_J \lesssim 22.5$ redshift distribution and produce stronger constraints on the luminosity evolution of the brightest galaxies.

The second issue addressed in this paper concerns the nature of the very blue galaxies identified at $B > 22.5$ ($R > 22$) by photometric studies (e.g. Tyson 1988). Of particular interest are the rapidly increasing numbers of objects with colours as blue or bluer than low-redshift star-forming irregulars such as NGC 4449 (Ellis 1983). Many of these are so-called 'flat-spectrum' objects, with continuum spectra approximated by $f_\nu = constant$. Spectral energy distributions of this form are invariant under redshifting, so their broad-band colours do not contain any indication of their redshift. However, as Cowie et al. (1988) have pointed out, standard nucleosynthesis arguments imply that the amount of metals produced by a population of star-forming galaxies with approximately flat spectra is directly related to their surface brightness on the sky. The number of galaxies observed in faint multiband studies to have near-flat spectra then suggests that such objects could have generated a significant fraction of the metals observed in present-day galaxies. The faint blue galaxies are therefore interesting either as a major star-forming epoch in normal galaxies if they are at moder-

ate-to-high redshift ($z \gtrsim 0.5$), or as an entirely new population of dwarf galaxies not seen locally if at low redshift ($z \lesssim 0.5$).

One limit on the redshifts of this population comes from *U*-band imaging by Guhathakurta, Tyson & Majewski (1990), who find that the overwhelming majority of faint blue galaxies have near-flat spectra in $U - B$ as well as at longer wavelengths. The lack of red $U - B$ colours indicates that the Lyman limit has not entered the *U* band and that therefore at most only a few per cent of the faint blue population could have redshifts greater than $z \sim 3$. Apart from this upper limit, however, redshift information for the faint blue galaxies has been lacking. Photometric redshift estimates based on broad-band colours are not possible due to the inherent properties of flat-spectrum objects, and the faintest available redshift surveys have produced but few examples because of the scarcity of such blue objects brighter than $B \approx 23$. Even the relatively large sample of galaxies brighter than $b_J = 22.5$ in the LDSS deep survey (Paper I) contains only seven examples with colours bluer than $b_J - r_F = 0.5$, similar to the flat-spectrum objects. Redshifts were obtained for four of the seven, however, and all had $z \lesssim 0.3$. This result is suggestive, but it could be argued that objects as bright as this are not necessarily representative of the much more numerous population of very blue objects found a magnitude or more fainter.

We have therefore undertaken a redshift survey of a sample of galaxies chosen to be representative of the faint blue population, using CCD photometry in *B*, *R* and *I* to select the bluest galaxies in the magnitude range $22 < R < 23$ and defining 'blue' in a number of ways according to various possibilities which warrant testing. In Section 3 we report the results of this survey, made using the Low Dispersion Survey Spectrograph (LDSS) on the Anglo–Australian Telescope (AAT). This work complements a recent survey by Lilly, Cowie & Gardner (1991) and Cowie et al. (1991, 1993) who report redshifts for a purely magnitude-limited sample to $B = 24$ without colour selection of blue objects.

We discuss the implications for galaxy evolution of this faint blue galaxy survey, and of the extensions to the original deep survey, in Section 4. Our conclusions are summarized in Section 5.

2 EXTENDING THE LDSS DEEP SURVEY

2.1 New observations

Of the 149 objects in the original LDSS deep redshift survey (Paper I), only 29 (19 per cent) were not identified. The unidentified fraction was, however, an increasing function of apparent magnitude, rising to a maximum of 25 per cent at the survey limit of $b_J = 22.5$. As it is expected that fainter objects will in general be at higher redshift, this may conceivably have resulted in a bias against high-redshift objects. More problematically, an alternative explanation might be that there was an inherent observational bias against detecting high-redshift galaxies, which was manifested as an increasing fraction of unidentified objects at fainter apparent magnitudes. As discussed in Paper I, the detectability of the common [O II] 3727-Å line in the unidentified spectra allowed us to rule out the possibility that *all* the unidentified objects lie in a high-redshift tail to the observed distribution. Nonetheless the observations were consistent, at the 90 per

cent confidence level, with as much as 15 per cent of the galaxy population lying in such a tail.

In order to tighten this constraint on the number of high-redshift objects brighter than $b_J = 22.5$, and hence the amount of luminosity evolution among $L \gtrsim L^*$ galaxies, we have therefore attempted to complete the survey of Paper I in two of the six zones (10.4 and 13.2) by re-observing the unidentified objects in the original samples. Additional objects, mostly selected according to the original survey criteria, were also observed. In order to obtain spectra with higher signal-to-noise ratios (S/N), particularly in the red, we have used a Thomson CCD as the detector for LDSS rather than the Imaging Photon Counting System (IPCS) – redward of 6300 Å (corresponding to [O II] 3727 Å at $z > 0.7$) this CCD has eight times the efficiency of the IPCS. In other respects the new observations, carried out over the three nights 1991 March 22–24, are very similar to those made for the original survey. LDSS was used in its high-dispersion mode to give a spectral resolution of 13 Å over a wavelength range of $\lesssim 3000$ Å in the region $\lambda\lambda 4300–7800$ Å, depending on the position of the object's slit on the focal plane mask. Each of the two zones was observed for a total of 18 500 s. The seeing for these observations was 1–1.5 arcsec. Reduction procedures followed those of Paper I.

The objects observed in each zone are listed in Table 1, which gives object identification (ID), position, b_J magnitude, $b_J - r_F$ colour, image classification as a star or galaxy, estimated redshift (*star* in this column means the object was identified as a star) and a quality class, Q, for the redshift. The IDs for the re-observed objects are the same as those given in Table 3 of Paper I, while the extra new objects have been given IDs which follow sequentially from the last IDs in the original samples. The magnitudes, colours and image classifications are derived from deep AAT plates scanned by the COSMOS measuring machine at the Royal Observatory, Edinburgh, and calibrated by deep CCD photometry (see Paper I for full details). Note that, as previously, no attention was paid to the image classifications in selecting the new objects, which generally are a magnitude-limited sample with $21 \leq b_J \leq 22.5$ (although some slightly fainter objects were included in zone 13.2). The redshift quality class, Q, is also defined as before: $Q = 1$ are the most reliable redshifts, confirmed by more than one spectral feature; $Q = 2$ are redshifts based on a single feature (usually [O II] 3727 Å or Ca H and K for galaxies, Mg I b band for stars); $Q = 3$ are spectra for which no redshift could be ascertained; $Q = 4$ are objects for which the spectra extend over too small a range of wavelengths for identification; $Q = 5$ are objects for which no spectrum was detected. As in Paper I, objects with $Q = 4$ or 5 are excluded from subsequent analysis. For the objects re-observed here, Table 1 gives in parentheses the Q classes from Paper I.

2.2 Results

The spectra of the 12 objects which had single-feature redshifts ($Q = 2$) or were unidentified ($Q = 3$) in the original survey and which were re-observed here are shown in Fig. 1. Of the two objects for which single-feature redshifts were claimed in Paper I, one (13.2.16) is found here to have $z = 0.339$ based on identification of [O II] 3727 Å, Ca H + K, Hβ and [O III] 4959 and 5007 Å. This is in good agreement

Table 1. Extensions to the LDSS deep redshift survey.

ID	R.A. (1950) Dec		b_J	$b_J - r_F$	S/G	z	Q
10.4.03	10 43 52.63	−00 00 59.2	21.74	0.72	s	0.276	2 (3)
10.4.04	10 43 48.52	−00 05 56.7	21.79	1.03	s	0.154	2 (3)
10.4.06	10 43 47.34	−00 02 17.8	22.32	2.11	s	star	1 (2)
10.4.23	10 43 51.88	−00 01 33.4	22.40	2.79	g	0.441	1 (3)
10.4.24	10 43 48.91	−00 03 01.3	22.48	2.00	g	star	1 (3)
10.4.25	10 43 44.76	−00 08 12.4	21.06	2.10	g	0.297	1
10.4.26	10 43 45.68	−00 02 35.8	21.26	1.38	s	0.323	1
10.4.27	10 43 51.89	−00 08 45.9	21.32	1.63	g	0.299	2
10.4.28	10 43 40.16	−00 07 52.2	21.33	1.58	g	0.394	2
10.4.29	10 43 49.92	−00 06 13.5	21.35	2.30	s	star	1
10.4.30	10 43 47.37	−00 04 08.9	21.53	0.75	g	—	3
10.4.31	10 43 47.52	−00 04 45.3	21.71	1.06	s	star	1
10.4.32	10 43 56.31	−00 04 23.3	22.00	2.21	g	0.439	1
10.4.33	10 43 43.22	−00 05 34.9	22.21	1.07	g	—	5
10.4.34	10 43 38.50	−00 07 34.2	22.35	1.54	g	0.230	2
10.4.35	10 44 02.65	−00 03 49.5	22.38	0.30	s	—	4
10.4.36	10 44 03.35	−00 02 02.6	22.40	—	g	—	4
10.4.37	10 43 53.86	−00 06 35.9	21.87	1.96	s	star	1
13.2.05	13 41 50.32	+00 00 27.3	21.95	2.17	s	star	1 (4)
13.2.11	13 42 06.59	+00 01 34.2	21.72	—	g	—	3 (3)
13.2.14	13 42 05.85	+00 03 41.5	21.82	1.65	g	—	3 (3)
13.2.15	13 41 59.17	+00 04 10.7	21.98	1.87	g	star	2 (3)
13.2.16	13 41 49.54	+00 00 46.7	22.04	1.39	g	0.339	1 (2)
13.2.17	13 41 52.15	+00 03 07.1	22.08	1.42	g	0.202	2 (3)
13.2.19	13 41 49.61	+00 02 49.7	22.10	1.51	g	0.638	1 (3)
13.2.23	13 41 59.64	+00 05 42.9	22.33	1.49	g	0.281	2 (3)
13.2.24	13 41 47.57	+00 07 23.7	21.16	1.01	s	—	3
13.2.25	13 41 56.23	+00 07 47.0	22.17	2.27	s	star	1
13.2.26	13 41 54.18	+00 03 26.0	22.41	0.64	s	0.598	2
13.2.27	13 41 58.68	+00 05 03.1	22.63	2.16	s	star	1
13.2.28	13 42 03.38	+00 01 03.0	21.33	1.60	g	0.391	2
13.2.29	13 41 53.04	+00 05 27.8	22.21	1.17	g	0.259	1
13.2.30	13 42 04.66	+00 03 56.0	22.27	0.96	g	—	4
13.2.31	13 41 56.94	+00 06 32.5	22.38	0.82	g	0.165	1
13.2.32	13 41 55.70	+00 08 28.9	22.49	1.42	g	—	5
13.2.33	13 42 00.71	+00 04 30.1	22.49	1.58	g	—	3
13.2.34	13 41 54.50	+00 06 12.3	22.68	2.02	g	star	1
13.2.35	13 41 48.52	+00 01 19.1	22.71	1.15	g	0.210	1
13.2.36	13 41 58.30	+00 04 46.9	22.75	1.54	g	0.537	1
13.2.37	13 42 06.65	+00 02 22.1	22.77	0.40	g	—	4

with the redshift of 0.340, based on [O II] 3727 Å alone, which was obtained in Paper I. The other object with a previous single-feature identification (10.4.06) was originally claimed to have a redshift of 0.237. However, it was also observed in the LDSS low-dispersion survey of faint compact objects (Colless et al. 1991, hereafter Paper II), where it was in fact found to be an M star, the only one out of eight objects common to the high- and low-dispersion surveys of Papers I and II where a disagreement of identifications was found. The spectrum obtained here clearly confirms the object as an M star, the original incorrect redshift being the result of inadequate spectral coverage in the red and mis-identification of a weak feature at 4610 Å as [O II] 3727 Å.

Ten of the re-observed objects had no identifications in Paper I (i.e. were $Q = 3$). Eight now have redshifts based on the new spectra shown in Fig. 1. Three of these new redshifts are based on more than one feature ($Q = 1$), while five rest on the identification of only a single feature or are otherwise uncertain ($Q = 2$). Two (10.4.24 and 13.2.15) are M stars, the others are galaxies with redshifts in the range $z = 0.154–0.638$. Their redshift distribution, along with that of the objects identified in Paper I, is shown in Fig. 2. The slight deficit of low redshifts among the new identifications is due to the fact that [O II] 3727 Å drops off the blue end of the spectral range (4300 Å) at $z \approx 0.15$. Apart from this differ-
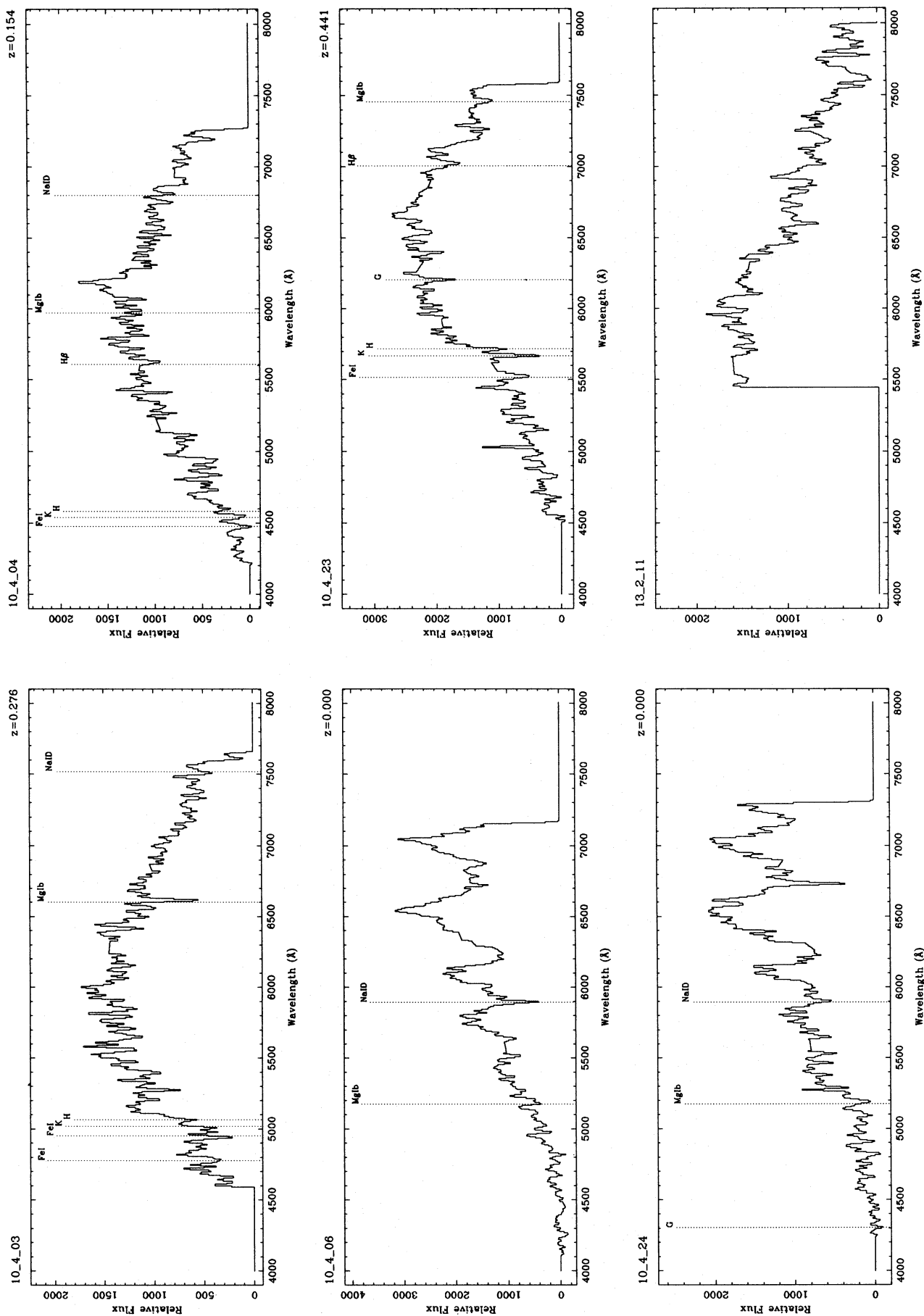
Figure 1. The spectra of the 12 objects classified $Q = 2$ or $Q = 3$ in the original deep survey of Paper I that were re-observed here. Spectral features used to obtain the redshifts are indicated. The residuals from the stronger night sky lines have been interpolated over.
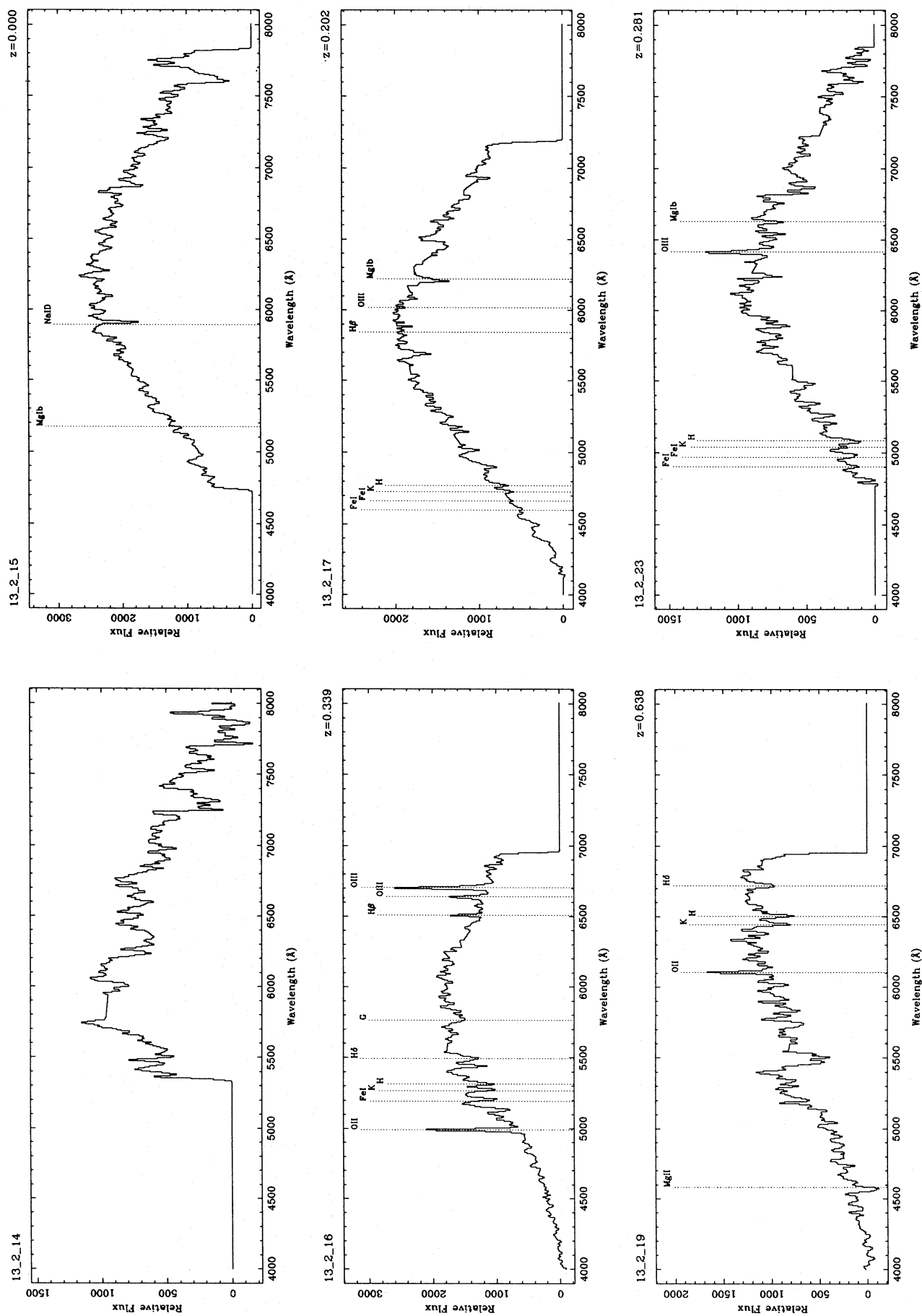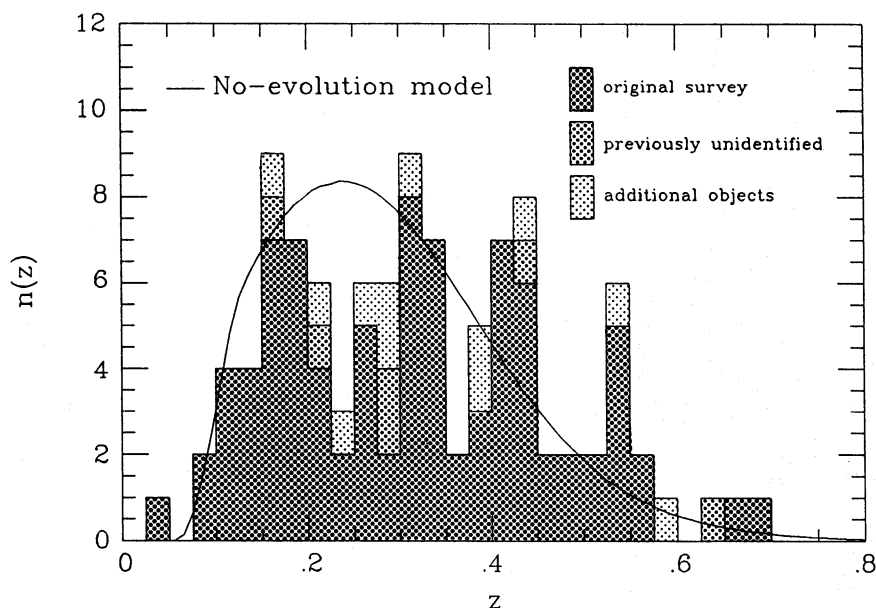
Figure 1 – *continued*

Figure 2. The redshift distribution for galaxies with $21 \leq b_J \leq 22.5$ from Paper I together with the redshifts obtained here for previously unidentified and newly added objects. The solid curve is the shape of the distribution predicted for no evolution of the galaxy population. The new redshifts are consistent both with the distribution from Paper I and the no-evolution prediction, except that there is a bias against redshifts less than $z \approx 0.15$, for which the [O II] 3727-Å emission line is blueward of the observed spectral range.

ence, the redshifts of the previously unidentified objects are consistent [at the 91 per cent level in a two-sample Kolmogorov–Smirnov (K–S) test] with being drawn from the redshift distribution of Paper I.

We have also obtained identifications for 19 additional objects with $21 \leq b_J \leq 22.8$. One of these additional objects (13.2.05) was in the original sample but the IPCS spectrum was too distorted to extract (i.e. $Q = 4$), so that the object was excluded from the analysis of Paper I. Five of the new objects (13.2.27, 13.2.34–37) have magnitudes in the range $22.5 \leq b_J \leq 22.8$, slightly fainter than the original survey sample. Of the additional objects, seven are found to be stars and 12 are galaxies with $z = 0.165$–0.598. Again the redshifts, which are shown in Fig. 2, are consistent (at the 69 per cent level, K–S test) with the redshift distribution of Paper I.

The results from these new observations considerably strengthen the conclusions of Paper I, since the incompleteness in the original sample for the two re-observed zones is reduced from 23 per cent (cf. 19 per cent overall) to just 4.5 per cent. The two remaining unidentified sources are both in one zone (13.2.11 and 13.2.14). The important point is that this fourfold reduction in incompleteness has *not* revealed any galaxies at redshifts higher than had been previously observed. As there is no reason to suppose these zones are unrepresentative, this implies that at most 4.5 per cent of galaxies brighter than $b_J = 22.5$ can have redshifts greater than $z = 0.7$. An even lower limit can be set if we assume that the unidentified galaxies are redshift-unbiased (at least out to $z \sim 0.9$). Our failure to identify these objects is, under this assumption, due to the low S/N of the observations, the intrinsically weak spectral features in the galaxies, or some other cause unrelated to the objects' redshifts. This assumption is supported by the fact that most of the previously unidentified objects in the original survey *can* be identified

with improved S/N, and are found to have the same redshift distribution as the rest. If the observed redshift distribution is indeed unbiased, then the observation that none of the sample of 104 identified galaxies in the range $21 \leq b_J \leq 22.5$ has $z > 0.7$ implies that the fraction of galaxies at redshifts higher than this in the underlying population must be less than 4 per cent at the 99 per cent confidence level, and less than 2 per cent at the 90 per cent level.

As Koo (1986, 1990) has shown, it is possible to match the faint blue number counts with galaxy evolution models that have only 'mild' luminosity evolution. Such models predict that 5–10 per cent of the galaxies to $b_J = 22.5$ should have $z > 0.7$, a prediction that would be only marginally inconsistent with the above results. A careful examination of the possibilities for survey incompleteness, line misidentifications and other biases is therefore required. We defer consideration of these points to Section 4, as the discussion applies also to the observations described in the following section, designed to test directly models such as 'mild' luminosity evolution which appear capable of reproducing both the redshift distribution to $b_J = 22.5$ and the faint number counts.

3 A FAINT BLUE GALAXY SURVEY

3.1 Photometry and survey sample

In Paper I and the extensions described above we studied samples to $b_J = 22.5$ with LDSS using multi-passband photometry from a number of deep prime-focus AAT photographic plates. Although a few very blue galaxies are contained in that catalogue, it is clear that a fainter limit is required to generate a significant sample whilst maintaining a good multiplex advantage and ensuring that the blue galaxies

are representative of the mean population at that magnitude. For convenience, we chose two of the deep survey zones (10.2 and 13.2) studied in Paper I.

The precision of the photographic magnitudes used in Paper I is insufficient to select accurately a sufficiently faint sample of blue galaxies. Accordingly, we have used independent, deep CCD photometry taken with the Isaac Newton 2.5-m telescope (INT) of the La Palma Observatory, kindly made available by K. Glazebrook and C. Collins. Standard *B*, *R* and *I* filters were used with an RCA CCD. Frames in each band were obtained at four positions within each LDSS zone. Each CCD field was 4.0×6.3 arcmin^2 and had 0.74-arcsec pixels. Some neighbouring frames overlapped, but others left gaps, so that coverage of each LDSS zone was not quite complete. The frames had typical integration times of 1000 s in *B*, 600 s in *R*, and 2000 s in *I*.

Image analysis was carried out with software supplied by M. Irwin employing the generic algorithms used by the Automated Photographic Measuring facility (APM). An image was deemed to be detected if it possessed at least four contiguous pixels with values more than the rms sky-noise above the local sky level. Image detection was carried out in each band separately, and 'total' magnitudes (Kron 1980) were determined. Because none of the frames was taken in photometric conditions, photometric zero-points were established through object-by-object comparisons with photographic photometry of the same fields derived from AAT prime-focus plates scanned with the COSMOS machine at the Royal Observatory, Edinburgh. The photographic photometry, and its calibration by CCD photometry, has been described in detail by Jones et al. (1991) and was used in the earlier LDSS surveys of Papers I and II. The photographic b_J and r_F magnitudes were transformed to the standard *B* and *R* systems using $B = b_J + 0.16(b_J - r_F)$ and $R = r_F + 0.07(b_J - r_F)$ (Jones et al. 1991); no transformation is necessary for the photographic *I* band.

The standard errors in the mean for the *B*, *R* and *I* zero-points obtained in these comparisons were 0.03, 0.02 and 0.08 mag respectively, the relatively large *I* error stemming from the poorer quality of the photographic photometry in this band. From the relatively small numbers of objects in the overlap regions belonging to more than one CCD frame we estimate internal rms errors for objects with $22 < R < 23$ of 0.08 mag in *R*, 0.09 mag in $B - R$ and 0.14 mag in $R - I$. Comparison of these zero-points derived from well-established photographic data with independent CCD zero-points subsequently obtained for these fields by K. Glazebrook (private communication) shows mean differences (CCD − photographic) and standard deviations across the eight CCD fields in the two LDSS zones to be −0.05 (±0.04) mag in *B*, +0.04 (±0.02) mag in *R* and +0.31 (±0.14) mag in *I*. The differences in *B* and *R* are negligible at the precision required for this study. The sense of the difference in *I* zero-points is that if the CCD rather than photographic zero-point were used then the $B - I$ and $R - I$ colours would be 0.3 mag *bluer* than we now suppose. We have not been able to resolve this disagreement, but, since we wish to use the colours to isolate objects bluer than certain limits, we prefer to err on the side of caution and so have remained with our photographic *I* zero-points.

Fig. 3 shows the $B - R$ versus *R* and $R - I$ versus *R* colour-magnitude diagrams for each zone, together with the

$B - R$ versus $R - I$ colour-colour diagrams. The effect noted by Tyson (1988) and by Lilly et al. (1991) is readily apparent – the lower envelope of both colour-magnitude distributions gradually shifts to bluer colours over a couple of magnitudes around $R = 22$. We chose to define our spectroscopic sample in the interval $22 < R < 23$, the practical limitations of LDSS spectroscopy in 1–2 night integrations being the major factor. We selected objects in the *R* band, rather than *B*, for several reasons. First, the INT *R*-band images are the deepest in terms of the S/N at a given excess count ratio, $\Delta N/N$, when compared to a standard no-evolution model. Secondly, the use of *R* as a base allows us to select further targets that are blue in $B - R$ or $R - I$ but not both. It may be that the expected high-redshift objects are a subset of the blue population in some form or other. Finally, in the configuration used with LDSS, the centre of the spectroscopic interval lies closer to *R* than *B*, and this has obvious advantages in the data reduction.

We defined 'blue' objects within this magnitude range in several ways. The principal criteria were that the objects have $B - R < 0.70$ *and/or* $R - I < 0.75$. A 'flat-spectrum' galaxy with $f_\nu \approx constant$ will have a colour of zero across all bands on the AB magnitude system [AB = $48.60 - 2.5 \log f_\nu$ (cgs units)], and colours of $B - R \approx 0.43$, $R - I \approx 0.22$ and $B - I \approx 0.65$ on the standard *BRI* system (Guhathakurta et al. 1990; Lilly et al. 1991). The selection criteria used will therefore include objects 0.3 mag redder than flat in $B - R$ and 0.5 mag redder than flat in $R - I$. Although the limiting *B* magnitude of the photometry ($B \sim 24.5$) does not affect the selected sample, the limiting *I* magnitude ($I \sim 23.5$) could mean that a few objects which are very blue in $R - I$ may have been omitted (see Fig. 3). It was for this reason, and because the *I* photometry had the largest zero-point uncertainty and rms internal error, that we opted to select the bluest objects in $B - R$ and $R - I$ independently.

Spectroscopic targets were chosen from the resulting photometric catalogue according to the following priorities (which we will refer to in subsequent discussion).

Priority 1. Objects for which $B - R < 0.70$ *and* $R - I < 0.75$; these are objects with spectra that are close to flat over optical wavelengths, having $B - I$ colours within 0.8 mag of those corresponding to $f_\nu = constant$. For comparison, the criterion used by Lilly et al. (1991) is equivalent to $B - I < 1.15$ (i.e. within 0.5 mag of a flat spectrum). We selected eight objects in this category, of which seven would also satisfy Lilly et al.'s criterion; the sampling rate was 40 per cent.

Priority 2. Objects for which $B - R < 0.70$ and either $R - I > 0.75$ or no *I* detection was recorded. These may be numerous in the *blue* counts but might be expected to be lower redshift galaxies undergoing strong star formation. We have five objects in this category; the sampling rate was 9 per cent.

Priority 3. Objects for which $R - I < 0.75$ and either $B - R > 0.70$ or no *B* detection was recorded. These could potentially be very high redshift objects if the red $B - R$ arises from the passage of the Lyman discontinuity through the *B* filter. However, much deeper imaging by Guhathakurta et al. (1990) suggests such objects should be very rare. Our relatively shallow *B* limit makes the absence of a *B* detection indicative of only a modestly red colour
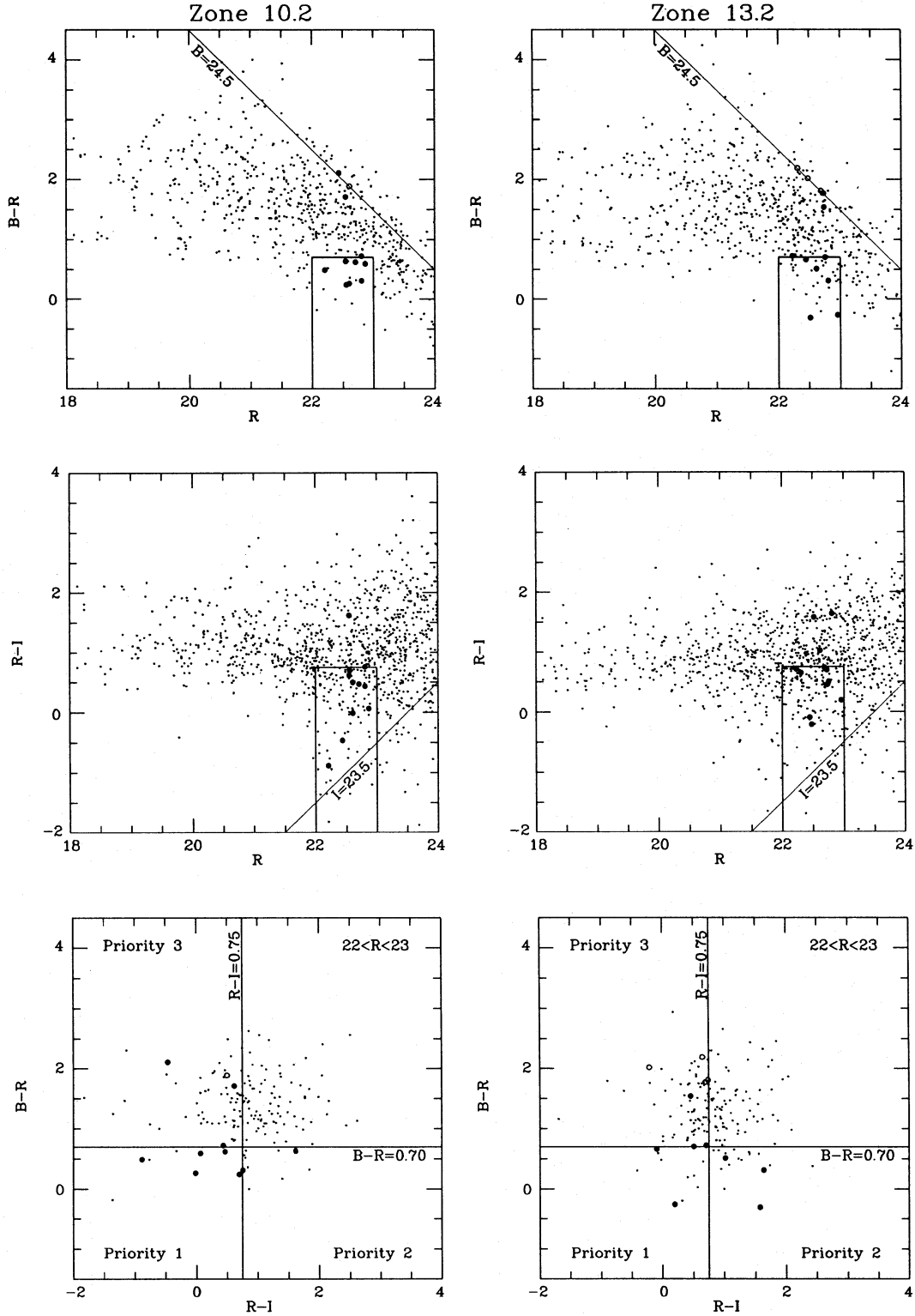
Figure 3. Colour-magnitude and colour-colour diagrams from which the spectroscopic sample for the faint blue redshift survey was selected. The figures on the left are for zone 10.2; those on the right are for zone 13.2. The small dots are the complete photometric samples for the zones; the large dots are the objects in the spectroscopic samples (large open dots are objects with no B magnitudes, assigned $B-R$ colours assuming $B=24.5$). The top two pairs of figures show the selection criteria in colour and magnitude on the $B-R$ versus R and $R-I$ versus R diagrams, and the limiting B and I magnitudes. The bottom pair of figures shows the priorities assigned the selected regions in the $B-R$ versus $R-I$ diagrams for objects with $22 < R < 23$.

$B - R > 1.5$, but we include this category for completeness. We have 10 objects in this category; the sampling rate was 4 per cent.

The selection criteria and priorities for the survey sample are summarized in Fig. 3.

3.2. Observations

Observations of the target objects were made using LDSS on the AAT with an uncoated 1024^2 Thomson CCD. Using the 164 Å mm^{-1} grism, this gave a FWHM resolution (measured from calibration lamp exposures) of 13 Å and a spatial resolution of 0.43 arcsec pixel^{-1}. Both the spatial resolution and throughput of the Thomson large-format CCD offer considerable improvements in performance over the IPCS used in Paper I. However, the performance shortward of 4500 Å with the uncoated CCD is poor and we adjusted our mask slit positions to yield a mean wavelength coverage $\lambda\lambda 4500$–7500 Å. The zone 10.2 centred at RA= $10^h43^m55^s.4$, Dec.= $+00°05'33''$ (1950.0) was observed for a total integration time of 41 800 s over two nights, 1990 February 27–28; the zone 13.2 centred at RA= $13^h41^m57^s.3$, Dec.= $+00°06'25''$ (1950.0) was observed for a total integration time of 32 200 s over the period 1990 April 24–28.

The data reduction methods proceeded largely as described in Paper I with one important simplification – the field distortion evident with the IPCS (introduced by its magnetic focusing coils) is eliminated when using a CCD. All frames were bias-subtracted and flat-fielded. The flat-field was constructed by taking a median of several undispersed sky exposures clipped to remove stars, and dividing the resulting vignetted image with a bicubic spline. The processed spectral images were registered and median-filtered

with 1.5σ-clipping, which adequately eliminated cosmic rays. Wavelength calibration was effected via interspersed helium lamp exposures. Third-order fits were obtained from typically eight arc lines, and gave residual wavelength errors of 0.3–0.7 Å (i.e. <0.1 resolution element) over the range $\lambda\lambda 4471.5$–7281.4 Å.

Overlaying the predicted position for the spectrum (from the source astrometry) revealed faint spectral continua in most (but not all) cases, and strong emission lines in some (an example is shown in Fig. 4). The spectra were extracted with the LEXT package as described in Paper I. An interactive fit to the slit profile was used to identify sky regions and to estimate the object position and extent. Sky-subtraction was typically achieved to an accuracy of 0.5–0.8 per cent. Weighted extraction of the object spectrum was used to obtain near-optimal S/N. The output spectra were rebinned to 3.0 Å pixel^{-1} but were not flux-calibrated. Identifications were made using a simple interactive LEXT procedure for finding and centroiding spectral features.

No spectra were detected at all for two objects in zone 10.2 and another two are absent in zone 13.2. All eight priority 1 objects were detected; one of the undetected objects was priority 2, the other three were priority 3. A spectrum could be absent for two reasons. First, the LDSS mask might have been slightly misaligned. During acquisition the precision of alignment is given by the residuals shared by three or more fiducial stars as compared to a direct 'white-light' image of the mask taken earlier (cf. Paper I). Occasional errors occur in the alignment procedure and these are necessarily more damaging for exceedingly faint sources. However, inspection of the location of the absent sources on their respective masks strongly suggests this is not the problem. More likely sources of error lie in the APM image analysis software, which at faint limits occasionally 'detects' spurious
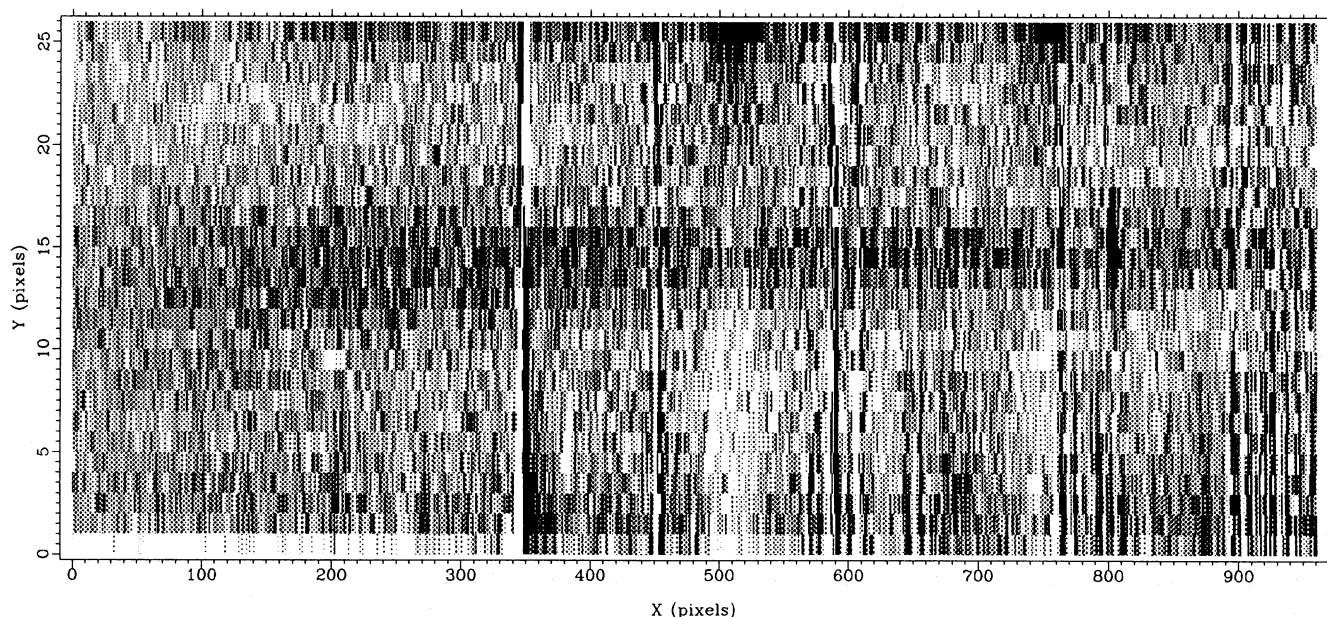

Figure 4. A subset of the sky-subtracted LDSS image for the field 10.2 showing the spectrum of object 10.2.14. The weak continuum has a spatial extent of about 2 arcsec (*Y* pixels 14–17), and runs from 4500 Å at low *X* to 7500 Å at high *X*. The object has a strong emission line clearly visible just below 7000 Å ($X \approx 800$). The remnants of several night-sky emission features are also apparent running across the spectrum.

Table 2. Faint blue redshift survey catalogue.

ID	R.A.	(1950) Dec	R	B−R	R−I	B−I	P	z	F	M_R
B10.2.01	10 43 54.53	+00 07 15.1	22.81	0.72	0.44	1.16	3	—	0	—
B10.2.02	10 43 54.27	+00 08 32.1	22.55	1.71	0.62	2.33	3	—	–	—
B10.2.03	10 43 55.52	+00 02 24.1	22.87	0.59	0.07	0.66	1	0.294	3	-16.8
B10.2.05	10 43 54.28	+00 03 24.8	22.21	0.49	-0.88	-0.39	1	0.283	2	-17.3
B10.2.06	10 44 12.40	+00 03 42.9	22.56	0.24	0.70	0.94	1	0.457	1	-17.9
B10.2.07	10 43 53.04	+00 04 26.7	22.71	0.62	0.47	1.09	1	—	0	—
B10.2.08	10 43 50.58	+00 04 50.0	22.81	0.31	0.76	1.07	2	—	–	—
B10.2.10	10 44 07.80	+00 05 50.9	22.61	≳1.89	0.50	≳2.39	3	0.450	1	-18.4
B10.2.11	10 44 02.32	+00 06 27.6	22.55	0.63	1.62	2.25	2	—	0	—
B10.2.13	10 44 08.29	+00 07 32.9	22.44	2.11	-0.46	1.65	3	0.341	2	-18.3
B10.2.14	10 44 05.32	+00 08 49.2	22.61	0.26	-0.01	0.25	1	0.868	1	-19.1
B13.2.01	13 41 46.66	+00 09 38.1	22.23	0.72	0.71	1.43	3	2.934	3	-23.1
B13.2.02	13 41 49.36	+00 10 48.9	22.76	0.70	0.51	1.21	1	—	0	—
B13.2.03	13 41 45.63	+00 06 14.3	22.45	0.66	-0.09	0.57	1	0.627	1	-18.9
B13.2.04	13 41 42.50	+00 08 18.4	22.96	-0.26	0.20	-0.06	1	0.297	1	-16.6
B13.2.05	13 41 42.20	+00 08 41.8	22.62	0.51	1.02	1.53	2	—	0	—
B13.2.06	13 41 43.76	+00 10 20.1	22.52	-0.31	1.58	1.27	2	—	0	—
B13.2.07	13 41 44.85	+00 07 31.0	22.81	0.31	1.64	1.95	2	—	0	—
B13.2.09	13 41 46.38	+00 06 50.2	22.74	1.54	0.46	2.00	3	0.667	1	-19.5
B13.2.10	13 41 42.34	+00 04 04.6	22.71	≳1.79	0.72	≳2.51	3	—	0	—
B13.2.11	13 41 47.28	+00 03 28.9	22.31	≳2.19	0.65	≳2.84	3	—	–	—
B13.2.13	13 41 39.95	+00 07 16.2	22.71	≳1.79	0.72	≳2.51	3	0.550	1	-19.0
B13.2.14	13 41 43.94	+00 02 43.9	22.48	≳2.02	-0.21	≳1.81	3	—	–	—

'objects' or (more commonly) identifies two merged objects as a single object, resulting in a spurious position centred on neither. In both these cases the object is very likely to have unusual colours. Because we have selected a sample with extreme colours, we are therefore also biased towards choosing spurious or confused objects.

3.3 Results

The spectroscopic catalogue is presented in Table 2 and the identified spectra are plotted in Fig. 5. Because the targets are exceedingly faint, the spectra are naturally very weak and noisy, even in $3-4\times10^4$ s integrations on the AAT. The features used in the identifications are indicated in each case. Cosmic rays, ghost images from the bright fiducial stars and other defects have been interpolated over, as have the residuals from night-sky lines. The ghost images were an unexpected problem apparently resulting from multiple reflections between the CCD window and the back side of the focal plane mask. They could be easily identified on the images as small faint doughnuts, leading to features like pairs of 'horns' when by mischance they fell on an object spectrum.

The spectroscopic catalogue of Table 2 gives ID number (prefixed by a 'B' to differentiate this survey from the previous one), position, R magnitude and B−R, R−I and B−I colours. Those objects not detected in B have listed approximate lower limits to their B−R and B−I colours, derived assuming a limiting B magnitude of 24.5. Table 2 also lists the observing priority P of the target (according to the categories of Section 3.1), and the number F of identified emission features used to determine the redshift (a zero in this column means a continuum was detected but no features, while a dash means no continuum or emission lines were detected).

Except in the case of the QSO B13.2.01, identified from Ly α, N v and C iv, spectra were identified using the [O ii] 3727-Å emission line, together with the [O iii] 5007-Å

line in B10.2.05 and B10.2.13 and both the 4959- and 5007-Å [O iii] lines in B10.2.03. No strong Hβ emission was found, although it may have been weakly detected in B10.2.06. The redshifts of B13.2.04 and B13.2.13 are based on a single line identified as [O ii] 3727 Å, but are supported by, respectively, the presence of Mg b-band absorption and the 4000-Å continuum break. The redshifts of B10.2.14 and B13.2.09 are based on single, very strong, emission lines (assumed to be [O ii]) unsupported by other features. The redshifts of both objects are sufficiently high that Mg ii 2798 Å would fall in the observed spectral range, although it is not detected in either case. Only B10.2.10 and B13.2.03 have redshifts based on an unsupported *weak* emission line, which again we assume to be [O ii]. In all cases where emission lines were found the continuum was also detected, and it was also detected in eight objects which had no identifiable features. As noted in the previous section, only four objects were not detected at all.

The R and B−I distributions of the survey objects with (i) measured redshifts, (ii) a detected spectrum but no redshift, and (iii) no detected spectrum are shown in Fig. 6. There is no apparent tendency for the undetected objects to be especially faint or to have colours more extreme than other objects in the sample, consistent with the suggestion made in the previous section that these objects are either spurious detections or have spurious positions. The objects with redshifts are not significantly brighter than those with detected spectra but no identifiable redshifts, although it is noteworthy that the objects that are bluest in B−I *have* been identified. The success rate for identifying redshifts from the detected spectra is six out of nine in zone 10.2 and five out of ten in zone 13.2, giving an overall success rate of just under 60 per cent. Six of the eight priority 1 objects and five of the ten priority 3 objects have redshifts; none of the five priority 2 objects could be identified.

The most significant result is that identifications have been secured for three-quarters of the priority 1 targets, i.e. those
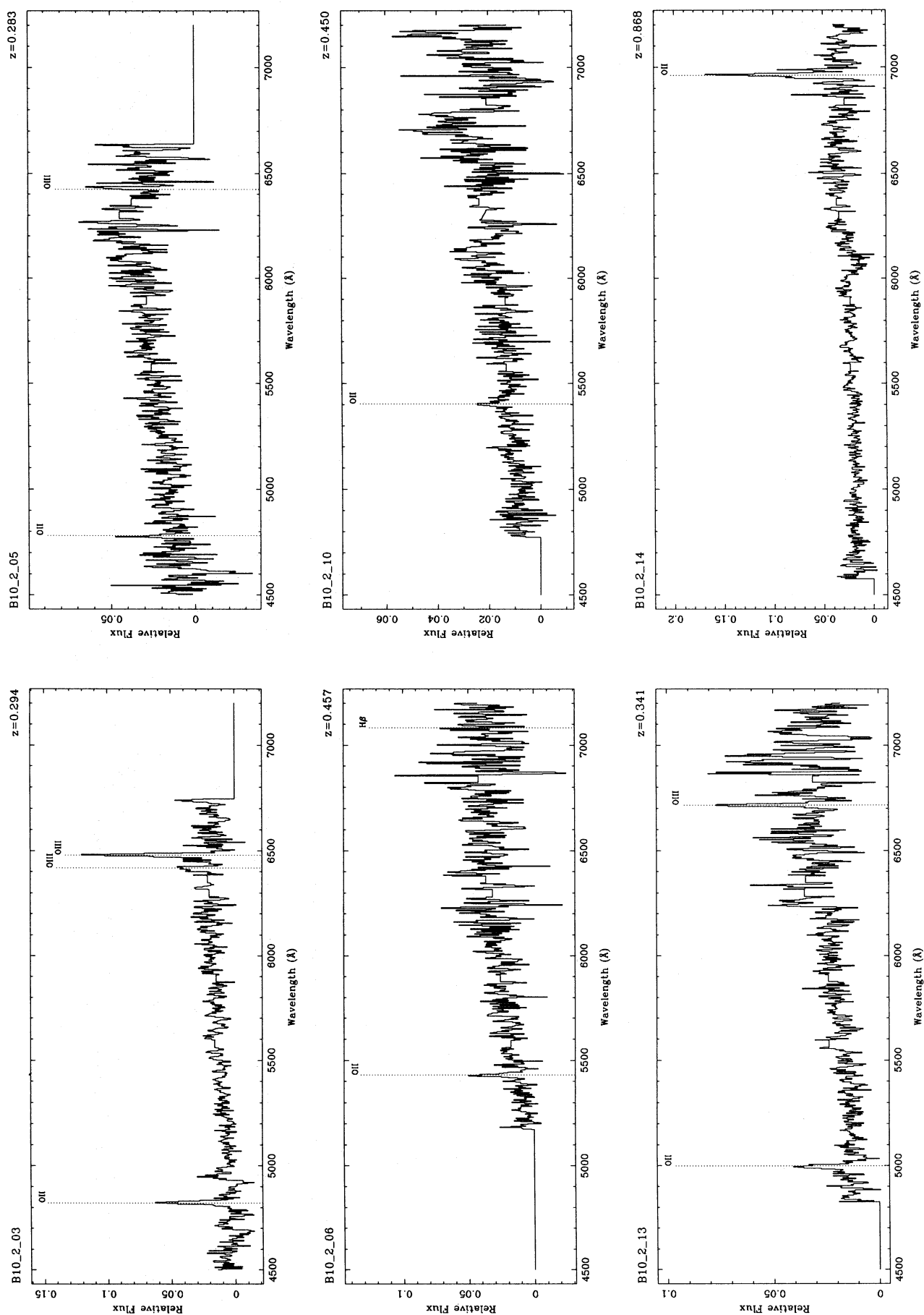
Figure 5. The spectra of the successfully identified objects in the faint blue redshift survey, with features marked. Defects and residuals from night-sky emission lines have been interpolated over.
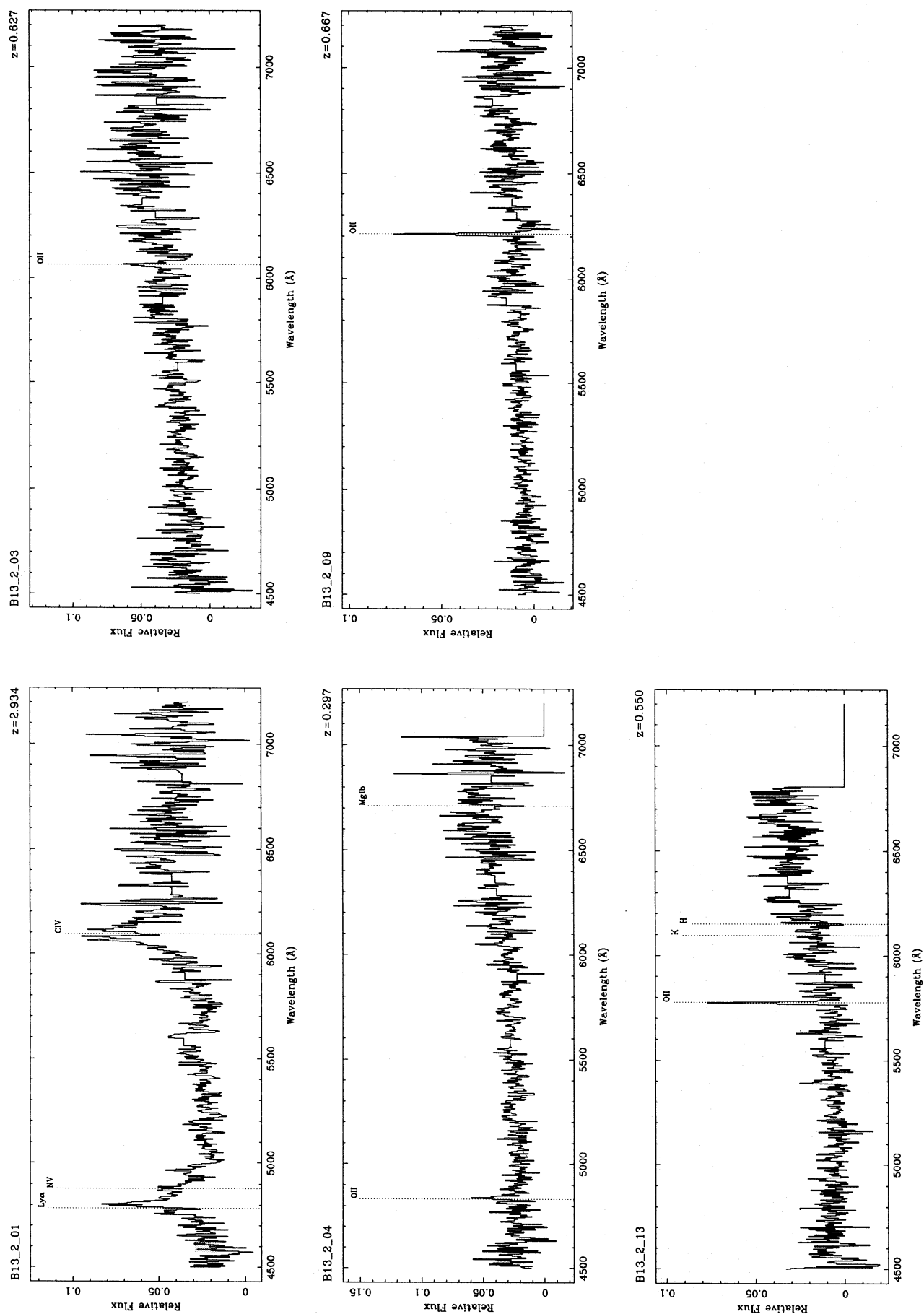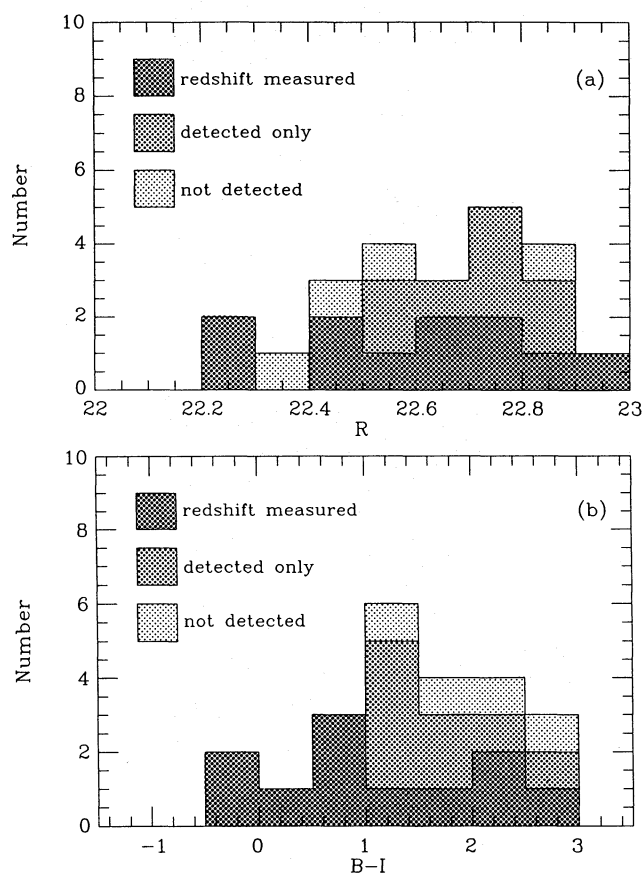
Figure 5 – *continued*

Figure 6. (a) The distribution in R of survey objects with (i) measured redshifts, (ii) a detected spectrum but no redshift, and (iii) no detected spectrum. (b) The $B - I$ distribution of survey objects in these same categories. For objects without B magnitudes the lower limit to $B - I$ assuming a limiting magnitude of $B = 24.5$ is used.

blue in both $B - R$ and $R - I$. Since these should be the most reliable flat-spectrum sources, their low mean redshift, $\bar{z} = 0.47 \, (\pm 0.10)$, is a strong argument against the majority of very blue galaxies as faint as $R = 23$ being at high redshift. We explore the implications of this result in detail in Section 4.2.

Excluding the QSO, the observed redshifts span the range $z = 0.28-0.87$. As Fig. 7 shows, the distribution of redshifts as a function of apparent magnitude for the blue, colour-selected galaxies in this survey ('faint blue survey') is entirely consistent with that found by Cowie et al. (1993; 'Hawaii survey') in their virtually complete survey of galaxies with $B < 24$. The galaxies in the faint blue survey have a median magnitude of $B_{1/2} = 23.3$ (almost a magnitude fainter than the survey of Paper I) and a median redshift of $z_{1/2} = 0.45$, while the Hawaii survey has $B_{1/2} = 23.1$ and $z_{1/2} = 0.31$. For such small samples this difference in median redshift is not significant – the two redshift distributions are consistent at the 49 per cent level in a two-sample K–S test. In as much as the range of redshifts (and the trend of mean redshift) is close to that expected in the case of no evolution of the galaxy population, both surveys are a natural extension to the larger surveys at brighter limits of Broadhurst et al. (1988) and Paper I (indicated in Fig. 7 as the 'fibre survey' and 'LDSS deep survey' respectively).

Fig. 8 shows the $b_J - r_F$ versus redshift distribution for both the new survey of faint blue galaxies and the LDSS deep survey of Paper I (including the extensions described in Section 2). The latter is a magnitude-limited survey to $b_J = 22.5$ while the former is colour-selected for blue galaxies in the range $22 < R < 23$. The figure also shows the colours, as a function of redshift, for unevolved galaxies of various spectral types. All six priority 1 objects for which redshifts were obtained are bluer than NGC 4449, one of the bluest known local galaxies. A 'flat-spectrum' galaxy with
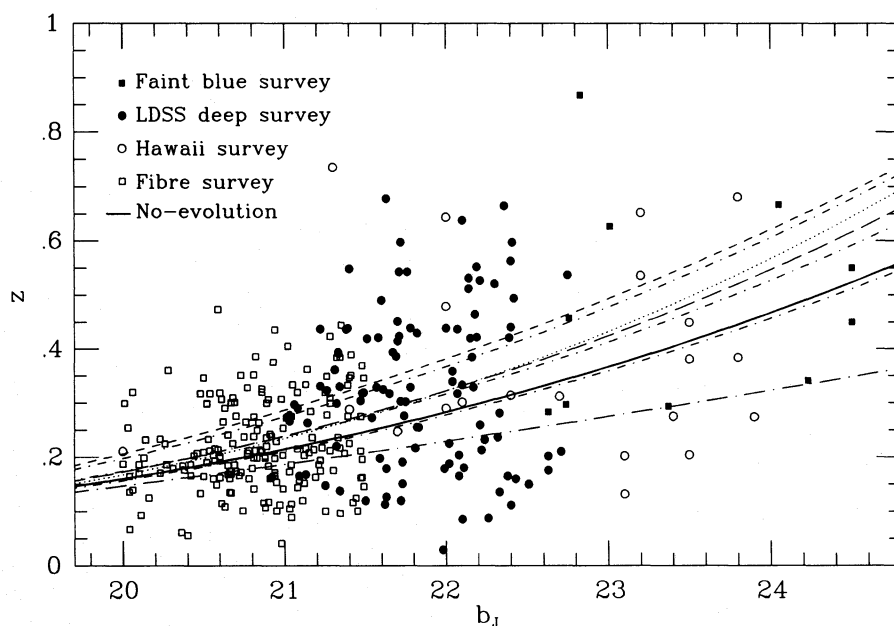

Figure 7. Redshift versus b_J magnitude. Galaxies from the faint blue survey are shown as filled squares; points marked as LDSS deep survey include the new redshifts reported in Section 2. Results from previous surveys are also shown. Galaxies from the faint blue survey that were not detected in B are shown at the lower limit of $b_J \approx 24.5$. The curves give median redshift versus b_J for various models: no-evolution (solid), late-type no-evolution (dots), mild luminosity evolution (short dash), burst model (long dash), three models with different merging rates (short dash-dot), and a model in which local dwarfs dominate (long dash-dot). The models are discussed in Section 4.2.
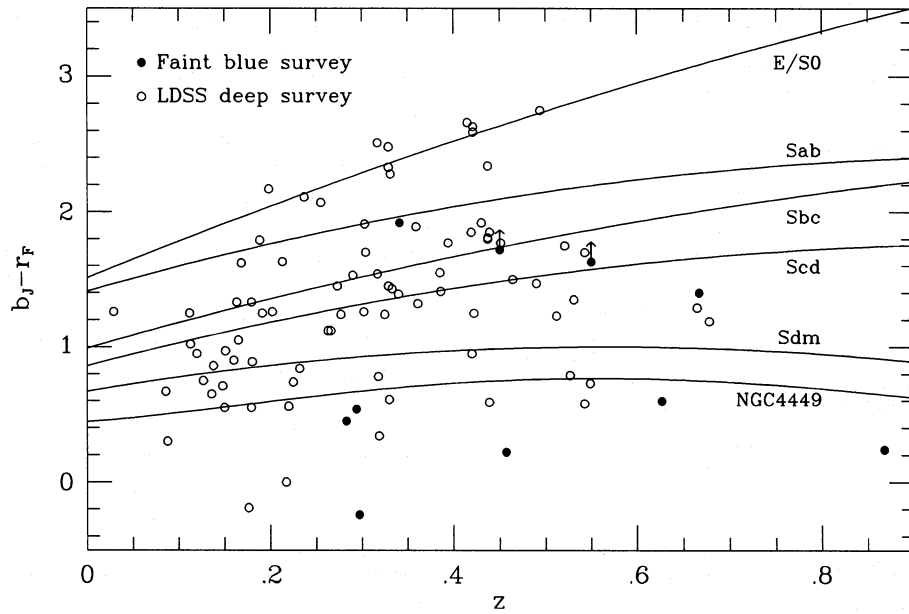
that the redshift distribution is declining monotonically and that our sample has no redshift bias, then we can conclude that no more than 4 per cent of galaxies brighter than $b_J \leq 22.5$ lie beyond $z = 0.7$ (at the 99 per cent confidence level). However, out of the 104 galaxies in the extended Paper I sample, many have single-line identifications ($Q = 2$). An important question is whether these, taken to be [O II] in all cases, might occasionally be due to a line of shorter wavelength (e.g. Mg II or Lyα) which would place the source at higher redshift. Only a small number of misidentifications would be needed to be compatible with a more traditional luminosity evolution picture (e.g. Koo 1986). Although this point was addressed by Broadhurst et al., where rest-frame co-addition of single-line spectra assuming [O II] identifications revealed the adjacent Balmer absorption sequence, we re-examine the question for the fainter samples in this paper.

In the two re-observed zones there remain four $Q = 2$ galaxies from the original Paper I samples whose redshifts still rest on a single emission line (10.4.19,20,21 and 13.2.22; other $Q = 2$ identifications are based on absorption features, usually Ca H+K). The mean redshift (and standard error in the mean) for these, assuming an [O II] identification, is $\bar{z} = 0.35$ (± 0.11), quite consistent with the mean redshift $\bar{z} = 0.34$ (± 0.03) obtained for the 27 secure $Q = 1$ galaxies in these zones. More importantly, for any plausible alternative identification, one might expect stronger secondary features to be present. The galaxies in question have lines at 3835, 5292, 5691 and 5300 Å. If each was Lyα, the spectral range would contain C IV or the Lyman limit. Similarly, if Mg II was the identification, [O II] would be expected in all but one. In fact, spectra are now available for several galaxies where Mg II can be seen (e.g. 13.2.19, cf. also Bergeron 1991); it is a weak feature, often in absorption. Similar conclusions can be drawn from the *IUE* spectra of spiral nuclei obtained by Ellis, Gondhalekar & Efstathiou (1982), where only the very bluest galaxy, NGC 4449, displays Mg II in emission. Similar arguments apply to the priority 1 sources in the faint blue galaxy survey of Section 3. Out of eight objects, two have $Q = 1$ redshifts and four have $Q = 2$ redshifts assuming [O II] identifications of features at 5430, 6962, 6064 and 4834 Å. Again, if these were Lyα then the spectral range would contain at least one of C IV or the Lyman limit; if Mg II, then two should also show [O II]. The spectrum of 10.2.14 allows only one of two extreme interpretations: the feature at 6962 Å must be either an extraordinarily strong Mg II line at $z = 1.488$ or a strong (but not unusual) [O II] line at $z = 0.868$, in which case the absence of any corresponding Mg II is a particularly convincing demonstration of that feature's weakness and our argument that most strong lines in our wavelength range can only be [O II].

Thus if there are high-redshift sources it seems clear they can only be those with *featureless* spectra. One could postulate that these occupy 'redshift windows' where no features fall in the LDSS spectral range. Our new extension of the Paper I survey probed to longer wavelengths in order to study this possibility. The two stubborn $Q = 3$ objects remaining in the original zones (i.e. excluding additional new sources surveyed) have been studied with adequate continuum S/N over 3700–7800 Å without detection of any strong features. The absence of [O II] and Lyα could imply redshifts for these objects in the range $1.1 < z < 2.0$. However, both are relatively bright ($b_J \leq 21.8$) and could

equally plausibly be low-redshift objects with weak features. They are not therefore obviously representative of any excess population seen in great abundance at fainter limits, although strictly we cannot eliminate the possibility that there are two sources with $1.1 < z < 2.0$ in the sample.

We now turn to the suggestion made by Phillipps, Davies & Disney (1990) and Yoshii & Fukugita (1991) that surface brightness selection effects, which are likely to be strongly redshift-dependent, preferentially eliminate the high-redshift luminous sources whose absence in our surveys is so puzzling. We would like first to emphasize a point that appears to have been misunderstood in this connection. Since we base our spectral target lists on the same catalogues that demonstrate the excess of faint galaxies, even if such biases are important *they cannot account for the origin of this population* – the objects making up the excess counts *must* be in the redshift survey samples. A redshift-dependent selection effect would simply exclude high-redshift objects from the number count catalogues in the first place, invalidating any comparison of redshift distributions between samples drawn from these catalogues and models that did not take into account this effect. Yoshii & Fukugita claim that neglect of just such a selection effect (rather than a genuine dearth of high-redshift galaxies) is the explanation for the observed lack of a high-redshift tail in our sample to $b_J = 22.5$. If their claim is correct it would allow bright galaxies to undergo strong evolution without turning up at high redshift in these surveys, *although the bulk of the faint blue galaxies would still have to be due to some other phenomenon.*

To examine this effect, we have explored various possibilities using the surface brightness dependent selection criteria originally developed by Ellis, Fong & Phillipps (1977) and used by King & Ellis (1985) to model the faint counts. We refer the interested reader to those papers for details. Briefly, galaxies are supposed to be of two morphologies: disc systems with exponential surface brightness distributions and spheroidal systems with de Vaucouleurs $r^{1/4}$-law distributions. These are populated in cosmological volumes with due regard to their luminosity functions and K-corrections, divided into five distinct spectral classes. In constructing observational catalogues, measuring machines like COSMOS and image processing algorithms normally impose a surface brightness limit and a minimum area limit when detecting sources. To mimic this effect on the distribution, each model galaxy is convolved with a Gaussian point-spread function and its isophotal size and magnitude are calculated to determine whether it meets the detection criteria.

Simplicity is the keynote here. Much of the information required to do a thorough job is not available. For example, we do not allow for intrinsic galaxy shapes nor departures from the simple surface brightness representations. A critical factor is the distribution of central surface brightnesses and galaxy sizes at a fixed luminosity. For disc systems we have adopted Freeman's (1970) empirical relationship, although we recognize there are populations that do not share it. For spheroidal systems we adopted Gudehus's (1973) correlations. We stress that our main goal is to explore, with the information at hand for luminous galaxies, whether their past evolutionary forms might be masked by such selection biases.

To exaggerate the possibility we take the extreme case where there is strong evolution in the counts arising from a large high-redshift tail in the distribution. This was implemented by endowing all galaxies with strong luminosity evolution from a Bruzual (1983) $\mu = 0.5$ model ($H_0 = 50$ km s^{-1} Mpc^{-1}, $\Omega = 1$). We then calculated the redshift distribution for a $b_{\rm J} = 21$–22.5 sample selected at various surface brightness limits imposing the COSMOS minimum area limit (1.2 arcsec^2) and a seeing of 1.0 arcsec FWHM. The results are summarized in Fig. 10.

An important verification of our results, not demonstrated in earlier studies, is that as we reduce the surface brightness level to very faint limits the distribution tends naturally to that calculated for the 'total' magnitude prediction (which uses a very different code). The high-redshift tail remains visible to all practical surface brightness limits including that adopted for our Paper I sample ($\mu_{b_{\rm J}} = 26.5$ arcsec^{-2}). The only visible effect of raising the threshold is a loss of galaxies near the peak of the redshift distribution. Since surface brightness does dim remarkably rapidly with redshift [$\propto (1+z)^4$], this result seems paradoxical at first. However, so far as distant sources are concerned, we have assumed evolution brightens the entire surface brightness profile in a self-similar way. The central peak thus remains significantly above the threshold even allowing for $(1+z)^4$ dimming. After convolution with the point spread function, the galaxies still remain larger than the minimum detection size, although they would probably appear as very blue stellar sources. Strong constraints on such a population to $b_{\rm J} = 23.5$ were recently provided by a separate LDSS survey of compact sources (Colless et al. 1991, Paper II). The loss of sources at intermediate redshifts occurs primarily because, for a given central surface 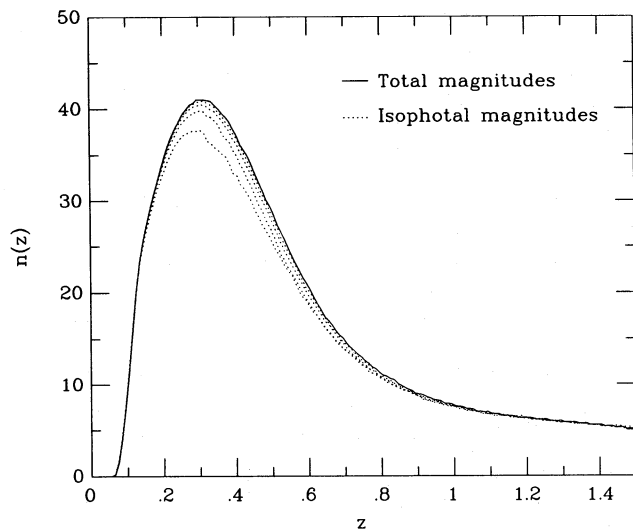brightness, disc systems must be smaller as one progresses to lower luminosities. At redshifts where evolution is not yet significant, these smaller galaxies are the first to fall below the minimum detection size.

If, as argued above, the absence of high-redshift sources does not arise from significant observational incompleteness or surface brightness selection, we can use the observed redshift distributions to place limits on the luminosity evolution of normal L^* galaxies. We find (see Section 2.2) that of galaxies brighter than $b_{\rm J} = 22.5$ no more than 2 per cent (at the 90 per cent confidence level) or 4 per cent (at the 99 per cent level) have $z > 0.7$. If we assume a very simple parametric form for luminosity evolution, letting the luminosity of all galaxies increase exponentially with z and resulting in Δm magnitudes of brightening by $z = 1$, we can establish the maximum values of Δm that are consistent with the above limits. We shall ignore the effect of luminosity evolution on the galaxies' colours so that our result will be independent of the evolutionary details. This leads us to obtain an upper limit on the amount of luminosity evolution that is slightly conservative (i.e. slightly too high), since any realistic model of luminosity evolution would tend to make the galaxies bluer, counteracting the effect of the K-corrections and so resulting in more galaxies being detected at higher redshifts. Using this very simple scheme, we obtain the benchmark figures that the 90 per cent confidence upper limit on the number of high-redshift galaxies is not consistent with *any* evolution of the most luminous galaxies, and that the 99 per cent upper limit is consistent with no more than 1.0–1.2 magnitudes of brightening by $z = 1$.

4.2 What are the faint blue galaxies?

Various models to explain the nature of the faint blue galaxies have been proposed, including fine-tuned general luminosity evolution (Koo 1986, 1990), an increasing frequency of bursts in star-formation activity (Broadhurst et al. 1988), merging-driven evolution (Guiderdoni & Rocca-Volmerange 1990b; Broadhurst, Ellis & Glazebrook 1992), and a new population of sub-luminous galaxies which underwent a burst of star formation at moderate redshifts and have since faded beyond detection (Cowie et al. 1991).

The crucial ingredient for understanding these objects is their redshift distribution, but, because they are so faint, no redshift information was available until recently for well-defined field samples. The faint blue survey described in this paper is the first to target specifically the population of objects at $R > 22$ which have near-flat spectra and colours bluer than those found in the bluest low-redshift galaxies. In this respect it complements the magnitude-limited survey of Cowie et al. (1991), which contained only two objects with flat or near-flat spectra between B and K (a flat-spectrum object has $B - K = 2.2$; Cowie et al. 1993) and no objects with $B - I$ colours bluer than those found locally (the bluest has $B - I = 1.1$; Lilly et al. 1991). It is therefore important to compare the survey results with the predictions the various models make for the redshifts of the blue population.

The most-studied of these models, and in principle the simplest, is that sometimes referred to as 'mild luminosity evolution' (Koo 1989, 1990; Guiderdoni & Rocca-Volmerange 1990a). The salient features of this model are: (i) that galaxies form at relatively high redshifts ($z_{\rm f} \gtrsim 5$) so that their recent evolution is mild, yielding redshift distributions

Figure 10. Model redshift distributions for a strongly evolving population of galaxies as sampled to $b_{\rm J} = 22.5$ assuming various surface brightness selection criteria. The solid line is for total magnitudes, and the dotted lines are for isophotal detection thresholds $\mu_{b_{\rm J}} = 29.5, 28.5, 27.5$ and 26.5 mag arcsec^{-2}, respectively, from top to bottom. The high-redshift tail is preserved for typical detection parameters (see text for details).

little different from the no-evolution case; and (ii) that a low-q_0 universe is required in order to provide sufficient volume at high redshift for the large numbers of galaxies in the faint number counts. We have argued in the previous section that such a model, at least as it applies to the most luminous galaxies, is at best marginally consistent with the dearth of high-redshift galaxies found in our $b_J \le 22.5$ survey. Using the data from the faint blue survey it is possible to test another, more clear-cut, prediction of this model.

As Koo (1990) has shown, a mild-evolution model can reproduce very nicely the main features of the observed colour–apparent magnitude distribution in $B - I$ and B, especially the sudden increase in the numbers of objects with near-flat spectra having $B - I < 1$ (see Koo's figs 1c and d). This good agreement is also seen in the photometric data on which our faint blue survey is based. Fig. 11(a) shows $B - I$ versus B for the CCD data described in Section 3.1 compared to the contours of the colour-magnitude distribution from a mild luminosity evolution model. The blue envelope of the $B - I$ distribution moves one magnitude bluewards, in both data and model, over the interval $B = 22$ to $B = 23$.

The observed distribution of $B - I$ with z is also generally well-matched by the mild-evolution model for magnitude-limited samples with $B < 22$, where the model has minimal evolution (Koo 1990, figs 1a and b). This is in accord with the observations of Paper I which show that the colour-redshift distribution is close to that expected if there were no evolution at all (see, e.g., Fig. 8). Only at fainter magnitudes can a decisive test of the model be made. One important prediction of the mild-evolution model is that the great majority of galaxies with $B - I \lesssim 1$ (i.e. very blue or close to flat) should have redshifts $z > 1$ (Koo 1990, figs 1a and c). This can be seen from Fig. 11(b), which shows colour-redshift trajectories for various galaxy types in the case of mild luminosity evolution. In the absence of photometric errors, we see that objects with colours bluer than $B - I = 1$ are virtually all at redshifts greater than $z = 1$. These objects would not necessarily have been seen in the survey of Paper I since, as Fig. 11(a) demonstrates, such objects are rarely brighter than $B = 22.5$.

The galaxies in the faint blue survey are shown in Figs 11(a) and (b) as the large squares. Six of the survey objects have $B - I < 1$ and all six are found to be at redshifts less than $z = 1$. This is in stark contrast to the prediction of the mild luminosity evolution model, which, since the estimated rms error in our $B - I$ colours is ~0.2 mag (Section 3.1), would predict that all but one or at most two of these six objects must lie at redshifts greater than $z = 1$. Only if we have grossly underestimated our photometric errors could we avoid the conclusion that these data rule out mild luminosity evolution as a viable explanation for the origin of the faint blue galaxies. This conclusion *cannot* be avoided by an appeal to cosmological surface brightness dimming, even if one ignores our argument in the previous section that this is not a significant effect; for if such dimming is invoked to remove the high-redshift galaxies from the observed samples, the model is no longer able to reproduce the observed excess of very blue galaxies at faint magnitudes, since this excess is entirely due to the galaxies at $z > 1$.

What of the other proposed explanations for the faint blue galaxies? All can accommodate the number counts in
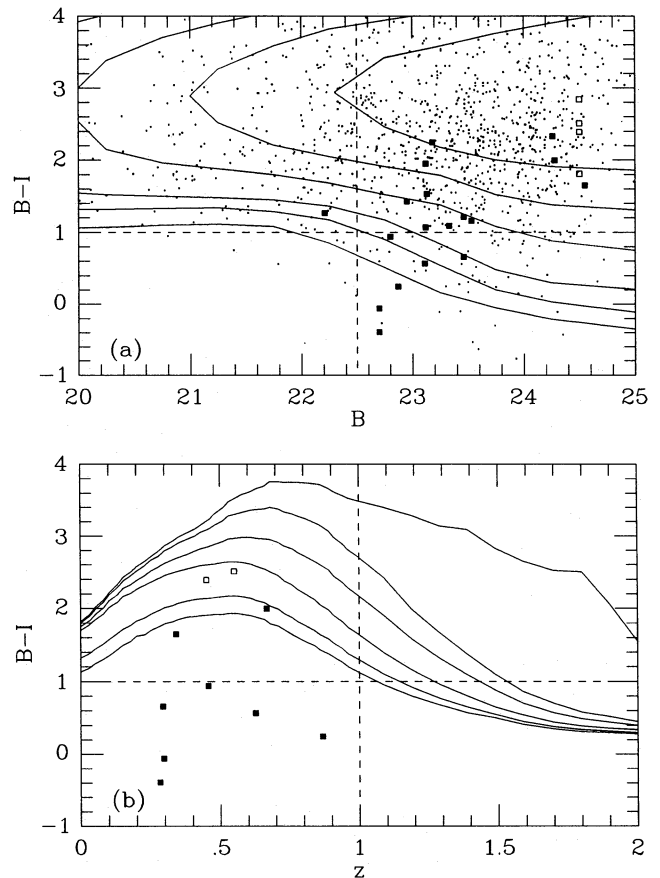

Figure 11. Colour-magnitude and colour-redshift diagrams comparing a mild luminosity evolution (low q_0, high z_f) model to observations. (a) $B - I$ versus B. The small dots are the photometric sample from which the galaxies of the faint blue survey were drawn. The survey objects are shown as squares (the open squares are those with no B detection, which are assumed to be at the limiting magnitude $B \approx 24.5$). The contours show the colour-magnitude distribution for a model with mild luminosity evolution. (b) $B - I$ versus z. The curves are the colour-redshift trajectories of various types of galaxy in a model with mild luminosity evolution. The squares are the objects with redshifts in the faint blue survey. Although the model satisfactorily reproduces the features of the colour-magnitude distribution, the colour-redshift trajectories imply that almost all the blue ($B - I < 1$) galaxies seen at faint ($B > 22.5$) magnitudes should be at high redshifts ($z > 1$); yet all six objects in the faint blue survey fulfilling these criteria are found to be at $z < 1$.

passbands from B to K, and can also be made consistent with the observed redshift distribution for $b_J < 22.5$. Are they consistent with the redshift distributions observed here and by Cowie et al. (1991) at fainter limits? Fig. 7 shows the distribution of galaxy redshifts with apparent magnitude in all the recent faint surveys along with the predicted run of median redshift with apparent magnitude for various models. Although the median does not do justice to the amount of information available brighter than $b_J = 22.5$, the paucity of data fainter than this requires a statistically robust characterization. As found at brighter limits, the no-evolution model (solid line) provides as good a match to the observations as any other. However (as expected from the discussions of this and the previous section), a model with mild

luminosity evolution (short dashes) has a median redshift that is marginally too high. Conversely, a model in which a population of *local* dwarfs dominates (long dash-dot) has too low a median redshift.

More successful is the Broadhurst et al. (1988) burst model, in which low-luminosity galaxies undergo short bursts of star formation resulting in a steepening of the faint end of the luminosity function with lookback time. The median redshift as a function of apparent magnitude shown in Fig. 7 (long dashes) corresponds to the preferred choice of parameters for this model (table 6, row 4, Broadhurst et al.) and, although somewhat higher than the no-evolution prediction, is consistent with the observations at all magnitudes. Also consistent are merging-driven evolutionary models such as those advocated by Rocca-Volmerange & Guiderdoni (1990b) and Broadhurst et al. (1992). The three merger models shown (short dash-dot) have, in the formalism of Broadhurst et al., $b = 4$ and $Q = 2, 4, 6$ from top to bottom respectively. Thus they have declining star-formation rates similar to a Bruzual $\mu = 0.25$ model and different merging rates such that the characteristic number density of galaxies is given by $\Phi^*(z) \simeq (1 + Qz)\Phi_0^*$ for $z < 1$. The model with least merging ($Q = 2$) predicts median redshifts that are too high, similar to those predicted by the mild-evolution model. More merging ($Q = 4, 6$) is required in order to keep the median redshift as low as is observed. The predictions of models in which a population of low-luminosity galaxies undergoes star formation at moderate redshifts and then fades beyond detection (Cowie et al. 1991) are not shown in Fig. 7, but can also be made to match the observations due to the considerable freedom one has in adding this ad hoc population.

One point worth noting is that the median redshift of late-type galaxies even without luminosity evolution (dots) is higher than the median redshift for all galaxies. This is due to the fact that the small K-corrections for such blue galaxies mean they can be seen to higher redshifts than redder objects whose large K-corrections render them unobservable sooner. Thus a sample selected for blue colours should, in simple luminosity-evolution models, yield higher redshifts than a purely magnitude-limited sample to the same depth. This does seem to be the sense of the difference between the median redshift found in our faint blue survey and that for the magnitude-limited survey of Cowie et al., although the samples are small. However, in both cases the median redshifts are somewhat *less* than those predicted without any evolution at all.

The absolute R-band magnitudes of the galaxies in the survey ($M_R = m_R - \mu - K_z - A_R$) can be approximated if we neglect absorption ($A_R \approx 0$) and estimate the K-corrections (K_z) by assuming that the galaxies in the survey have spectral energy distributions (SEDs) which can be approximated either by that of some low-redshift galaxy type or by $f_\nu = constant$. The $B - R$ colour and redshift of the galaxy can then be compared to the redshifted colours of standard galaxy SEDs (without evolution), and an approximate spectral type interpolated. The redshift and spectral type then yield an estimate of the R-band K-correction for the galaxy (as given by Metcalfe et al. 1991). For galaxies with colours as blue or bluer than a flat-spectrum galaxy (for which $B - R \approx 0.43$, independent of redshift) we use the K-correction appropriate to $f_\nu = constant$, namely $K_z = -2.5$

$\log(1 + z)$. Table 2 gives values of M_R estimated in this fashion (assuming $H_0 = 100$ km s^{-1} and $q_0 = 0.5$) for all the survey objects with redshifts. For the single QSO (B13.2.01) at $z = 2.934$ the K-correction (see Koo & Kron 1988) is essentially zero, giving $M_R \approx -23.1$.

All the galaxies have absolute magnitudes in the range $M_R = -19.5$ to -16.5. The characteristic absolute magnitude in the field at low redshift is $M_R^* \approx -21$, so that all of these blue objects are significantly fainter than L^*, with the faintest having intrinsic luminosities of $0.02L^*$. Comparing this to the luminosity functions given for different galaxy types by Binggeli et al. (1988), we see that the faintest objects lie in the range of absolute magnitude marking the change-over from normal bright galaxies (E, S0 and Sp) to dwarfs and irregulars (dE, Im and BCD). It is therefore plausible that we are seeing amongst the brightest dwarf galaxies the tail-end at low redshift of a star-forming phase whose manifestation in the rest of the dwarf galaxy population, and at higher redshifts, accounts for the very large numbers of blue galaxies observed at fainter magnitudes. On the other hand, two of the flat-spectrum objects are at higher redshifts (0.627 and 0.868) and are only two magnitudes fainter than L^*, so that their luminosities (at least during this star-forming phase) are not those of dwarf galaxies.

The small numbers of objects in the present sample are clearly not sufficient to distinguish directly between scenarios involving bursts of star formation peculiar to dwarf galaxies (e.g. Babul & Rees 1992) or those associated with more general merging activity in hierarchical cosmologies (White & Frenk (1991) and Lacey & Silk (1991)). Two promising approaches to discriminating between these cases are K-band selected redshift surveys and high-resolution multicolour imaging. Broadhurst et al. (1992) argue that a faint K-selected redshift survey would have a median redshift *less* than the no-evolution prediction in a merging-dominated scenario, while a model in which a new population of dwarfs are added to a mildly evolving normal population would retain a long tail to higher redshifts. At redshifts of $z \sim 0.3$, ground-based imaging in multiple passbands at high resolution (~ 0.5 arcsec) offers the possibility of mapping the location of star formation within these objects and of detecting possible merger candidates. Giraud (1992) has already imaged a small sample of faint flat-spectrum galaxies in V and I and finds a variety of morphologies, including compact and irregular objects and double or multiple systems.

5 CONCLUSIONS

We have presented the results of two new redshift surveys carried out with the Low Dispersion Survey Spectrograph (LDSS) on the Anglo-Australian Telescope.

The first is an extension of our earlier LDSS deep survey (Paper I), in which we have re-observed two of the original survey zones and reduced the 19 per cent incompleteness in redshift identifications to just 4.5 per cent. We have also obtained redshifts for 19 new galaxies in these zones, increasing the total number of redshifts in the survey to 104. We confirm the lack of a high-redshift tail to the observed redshift distribution, which was one of the major results of Paper I. With the much lower level of incompleteness we are

able to tighten the constraints on the amount of luminosity evolution in bright $(L \gtrsim L^*)$ galaxies. We conclude that *at most* 4.5 per cent of galaxies brighter than $b_J = 22.5$ can have redshifts greater than $z = 0.7$. If our redshift sample is unbiased (as the reduction in incompleteness with improved S/N suggests), then we infer that the fraction of $b_J \leq 22.5$ galaxies at $z > 0.7$ is less than 2 per cent at the 90 per cent confidence level and 4 per cent at the 99 per cent level. The former figure is consistent with no evolution in the luminosity of bright galaxies, but inconsistent with *any* significant amount of luminosity evolution. The latter figure is consistent with no more than 1.0–1.2 magnitudes of luminosity evolution by a redshift of $z = 1$. These results are only marginally consistent with 'mild' luminosity evolution models having low q_0 and a high redshift of galaxy formation, $z_f > 5$. We have examined the effect of surface brightness dimming on the observed redshift distribution, and conclude that it does *not* lead to a significant bias against observing high-redshift galaxies in our surveys.

The second redshift survey reported here is specifically aimed at the remarkable population of faint blue galaxies whose colours are bluer than those of any present-day galaxy and indicative of spectra that are close to flat in f_ν. These objects are apparent in the observed colour–magnitude diagrams of galaxies fainter than about $R = 22$. We have carried out a spectroscopic survey of a sample of 23 faint galaxies in the interval $22 < R < 23$ that have blue colours in one or both of $B - R$ and $R - I$. We are able to identify the redshift for 11 of these objects and, most significantly, for the bluest six galaxies (all those with $B - I < 1$) among the eight priority 1 objects for which *both* $B - R \leq 0.70$ and $R - I \leq 0.75$. Apart from one QSO, all the identified objects are galaxies with redshifts in the range $0.3 < z < 0.9$. The median depth of this blue-selected survey, $B_{1/2} = 23.3$, is close to that of the purely magnitude-limited survey of Cowie et al. (1991), for which $B_{1/2} = 23.1$. The median redshifts found in the two surveys $(z_{1/2} = 0.45$ and 0.31 respectively) are consistent within the errors for such small samples; the sense of the difference in median redshift is that expected between blue-selected and colour-unbiased samples. The distribution of redshifts with apparent magnitude for both surveys is consistent with no-evolution models, and thus provides an extension to $B \approx 24$ of the result of the larger survey to $b_J = 22.5$ described above and in Paper I.

A detailed comparison of the results of this survey with the predictions of mild luminosity evolution (low q_0, high z_f) models allows us to rule out such models as an explanation for the faint blue galaxy population. One of the strongest predictions of mild-evolution models is that the galaxies with $B - I < 1$ observed fainter than $B \sim 22.5$ should *almost all* be at redshifts greater than $z = 1$. We find, however, that we can identify the redshifts of all six galaxies in our survey meeting these criteria, and that all six have $z < 1$. Only one or at most two of these objects can have their blue colours explained away as being due to photometric errors – the rest must have genuinely near-flat spectra and so should be at high redshift according to the mild-evolution model. The failure of the model to explain the observed redshifts *cannot* be avoided by appealing to surface brightness biases, since if high-redshift objects were hidden from observation by some such effect the model would be unable to reproduce the very blue galaxies seen in the photometric data.

The absolute R magnitudes of the identified galaxies with near-flat spectra range from $M_R = -19$ to -16.5, i.e. from $0.15L^*$ to $0.02L^*$. The faintest objects thus have luminosities similar to those of bright dwarf (dE, Im or BCD) galaxies or the faintest normal E, S0 or Sp galaxies (Binggeli, Sandage & Tammann 1988). The brightest, at least while the star-formation activity reflected in their colours persists, are brighter than the brightest dwarfs and comparable to normal present-day galaxies. The current observations do not allow us to discriminate between evolutionary models which explain the low redshifts of faint blue galaxies by invoking merging activity (e.g. Rocca-Volmerange & Guiderdoni 1990) and those which postulate a new population of star-forming dwarfs (Cowie et al. 1991). This will require new and more extensive observations: in particular, infrared-selected redshift surveys and high-resolution multicolour imaging.

REFERENCES

Babul A., Rees M. J., 1992, MNRAS, 255, 346
Bergeron J., 1991, ESO Messenger, 62, 16
Binggeli B., Sandage A., Tammann G. A., 1988, ARA&A, 26, 509
Broadhurst T. J., Ellis R. S., Shanks T., 1988, MNRAS, 235, 827
Broadhurst T. J., Ellis, R. S., Glazebrook K., 1992, Nat, 355, 55
Bruzual G., 1983, ApJ, 273, 105
Colless M. M., Ellis R. S., Taylor K., Hook R. N., 1990, MNRAS, 244, 408 (Paper I)
Colless M. M., Ellis R. S., Taylor K., Shaw G., 1991, MNRAS, 253, 686 (Paper II)
Cowie L. L., Lilly S. J., Gardner J. P., McLean I. S., 1988, ApJ, 332, L29
Cowie L. L., Songaila A., Hu E. M., 1991, Nat, 354, 460
Cowie L. L., Gardner J. P., Hu E. M., Wainscoat R. J., Hodapp K. W., 1993, ApJ, submitted
Efstathiou G., Bernstein G., Katz N., Tyson J. A., Guhathakurta P., 1991, ApJ, 380, L47
Ellis R. S., 1983, in Jones B. J. T., Jones J. E., eds, The Origin and Evolution of Galaxies. Reidel, Dordrecht, p. 255
Ellis R. S., Fong R., Phillipps S., 1977, MNRAS, 181, 163
Ellis R. S., Gondhalekar P., Efstathiou G., 1982, MNRAS, 201, 223
Freeman K., 1970, ApJ, 160, 811
Giraud E., 1992, A&A, 257, 501
Gudehus D. H., 1973, AJ, 78, 583
Guhathakurta R., Tyson J. A., Majewski S., 1990, ApJ, 357, L9
Guiderdoni B., Rocca-Volmerange B., 1990a, A&A, 227, 362
Guiderdoni B., Rocca-Volmerange B., 1990b, MNRAS, 247, 166
Jones L. R., Shanks T., Fong R., Ellis R. S., Peterson B. A., 1991, MNRAS, 249, 481
King C. R., Ellis R. S., 1985, ApJ, 288, 456

1C91.....261.SARNM3991

M. Colless et al.

Koo D. C., 1986, ApJ, 311, 651
Koo D. C., 1989, in Frenk C. S. et al., eds, The Epoch of Galaxy Formation. Kluwer, Dordrecht, p. 71
Koo D. C., 1990, in Kron R. G., ed., Evolution of the Universe of Galaxies. ASP Conf. Ser. Vol. 10, p. 268
Koo D. C., Kron R., 1988, ApJ, 325, 92
Koo D. C., Kron R. G., 1992, ARA&A, 30, 613
Kron R., 1980, ApJS, 43, 305
Lacey C., Silk J., 1991, ApJ, 381, 14
Lilly S. J., Cowie L. L., Gardner J. P., 1991, ApJ, 369, 79
Metcalfe N., Shanks T., Fong R., Jones L. R., 1991, MNRAS, 249, 498
Phillipps S., Davies J. I., Disney M. J., 1990, MNRAS, 242, 235
Tyson J. A., 1988, AJ, 96, 1
White S. D. M., Frenk C. S., 1991, ApJ, 379, 52
Yoshii Y., Fukugita M., 1991, in Shanks T. et al., eds, Observational Tests of Cosmological Inflation. Kluwer, Dordrecht, p. 267
Yoshii Y., Peterson B. A., 1991, ApJ, 372, 8